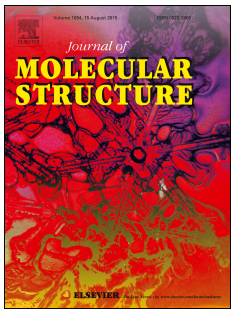

Synthesis, characterization, structural-activity relationship and biomolecular interaction studies of heteroleptic Pd(II) complexes with acetyl pyridine scaffold

Nikita J. Patel, Bhupesh S. Bhatt, Pankajkumar A. Vekariya, Foram U. Vaidya, Chandramani Pathak, Juhi Pandya, Mohan N. Patel

PII: S0022-2860(20)31127-3

DOI: https://doi.org/10.1016/j.molstruc.2020.128802

Reference: MOLSTR 128802

To appear in: *Journal of Molecular Structure*

Received Date: 16 April 2020

Revised Date: 18 June 2020

Accepted Date: 30 June 2020

Please cite this article as: N.J. Patel, B.S. Bhatt, P.A. Vekariya, F.U. Vaidya, C. Pathak, J. Pandya, M.N. Patel, Synthesis, characterization, structural-activity relationship and biomolecular interaction studies of heteroleptic Pd(II) complexes with acetyl pyridine scaffold, *Journal of Molecular Structure* (2020), doi: https://doi.org/10.1016/j.molstruc.2020.128802.

Nikita J. Patel: Conceptualization, Methodology, Software, Formal analysis, Validation, Investigation, Resources, Writing- Original draft **Bhupesh S. Bhatt**: Software, Validation, Conceptualization, Writing- Review & editing, Resources **Pankajkumar A. Vekariya**: Software, Data Curation **Foram U. Vaidya**: Investigation, Data Curation **Chandramani Pathak**: Resources **Juhi Pandya**: Investigation, Data Curation **Mohan N. Patel**: Writing- Original draft, Writing- Review & editing, Supervision

Synthesis, characterization, structural-activity relationship and biomolecular interaction studies of heteroleptic Pd(II) complexes with acetyl pyridine scaffold

Nikita J. Patel[1], Bhupesh S. Bhatt[1], Pankajkumar A. Vekariya[1], Foram U. Vaidya[2], Chandramani Pathak[2], Juhi Pandya[3] and Mohan N. Patel*[1]

[1]Department of Chemistry, Sardar Patel University,
Vallabh Vidyanagar–388 120, Gujarat (INDIA)
*Phone number: (+912692) 226856*218*
Corresponding address: jeenen@gmail.com

[2]Department of Cell Biology, School of Biological Sciences and Biotechnology,
Indian Institute of Advanced Research, Koba Institutional Area,
Gandhinagar-382007, Gujarat (INDIA)

[3]Department of Biosciences, Sardar Patel University,
Vallabh Vidyanagar, Gujarat, (INDIA)

Abstract

A series of substituted hydrazinyl pyridine based Schiff base ligands (L^1-L^6) and corresponding palladium(II) complexes were synthesized and characterized by conductivity measurement, ^{1}H NMR, ^{13}C NMR and liquid chromatography mass spectrometry (LC-MS). Synthesized compounds were screened against various biological activities. UV-Vis spectroscopy, fluorescence spectroscopy, viscosity measurement, and molecular docking studies were used to determine the binding mode between complexes and HS-DNA, which suggest intercalation mode of DNA binding. The protein binding study of complexes was evaluated by UV-visible spectroscopy. Antibacterial activity of the complexes was screened against two Gram (+ve) and three Gram (-ve) bacteria and the result shows that all complexes are more effective against microorganisms than their respective ligands. The cytotoxicity of the synthesized compounds was tested against brine shrimp and *S. pombe* cell. The LC_{50} values of the ligand and complexes are found in the

range of 9.24-14.12 µg/mL and 5.68-7.94 µg/mL, respectively. The DNA cleavage activity of metal complexes was performed using agarose gel electrophoresis. All compounds were tested for anticancer activity against human colorectal (HCT-116) cancer cell lines. The result shows that all the compounds exhibited effective cytotoxicity against the tested cell line.

Keywords: Mixed-ligand Pd(II) complexes, SAR, Protein binding, Cell line study

1. Introduction

The success of cisplatin in cancer treatment led the foundation of metal-organic, organometallic complexes, and inorganic compounds in modern medicinal chemistry [1-7]. Various factors are responsible for the increasing incidence of cancer, of which modernization of our society is a major one. In cancer treatment, resistance to drugs is one of the most significant problems [8, 9]. Several platinum drugs are used for the treatment of cancer, but the side effects connected with the usage of these drugs considerably limit their application [10]. Thus, transition metal like titanium, iron, osmium, rhodium, iridium, palladium, and coinage metal ions have been considered as alternatives to platinum based metallodrugs due to the cytotoxic properties of some of their compounds [11].

Effective biological activity of palladium(II) and platinum(II) complexes have attracted significant attention in the research area [9, 12]. The interest in platinum(II) and palladium(II) complexes containing S, S-, N, N- and O, S-donor have increased in nowadays with the desire to synthesize antitumor drugs having reduced toxicity than cisplatin and its analogues [13]. Anticancer agents have resulted in the development of a large number of palladium(II) complexes with nitrogen donor ligands, such as various alkyl and aryl substituted amines and imines, pyridine and pyrimidine derivatives, in which some of exhibit effective antitumor properties both *in vivo* and *in vitro* [14].

Schiff base ligands are mostly applied in coordination chemistry and it can coordinate with a large number of 3d, 4d, 5d transition metals [15]. Palladium is an important metal in medicinal research due to significant similarities in the coordination chemistry with platinum [16]. The initial way for cancer therapy will be metallodrugs started in the interaction between DNA and coordination complexes. These include three main

interactions between DNA and metal complexes: intercalation, groove binding, and electrostatic interaction [17, 18].

In continuation of our earlier work [19], six new hydrazinyl pyridine based Schiff base and their mixed-ligand palladium(II) complexes were synthesized and characterized. Synthesized compounds were screened against various biological activities.

2. Experimental section

2.1 Chemicals and materials

Commercial grade solvents and reagents were used without further purification. Sodium tetrachloropalladate (II) was purchased from S.D. fine chem. Ltd (SDFCL). 2-Acetyl pyridine, 2-hydrazinopyridine, 2-chlorobenzaldehyde, 2-bromobenzaldehyde, 4- chloro benzaldehyde, 4-bromo benzaldehyde, 4-flourobenzaldehyde, 4- methylbenzaldehyde, Hearring sperm HS-DNA and bovine serum albumin (BSA) were purchased from sigma aldrich chemical co. (India). Nutrient Broth (NB), agarose, ethidium bromide (EtBr), tris-acetate-EDTA (TAE) and bromophenol blue were purchased from Himedia (India). The solvents used for spectral measurements were of spectroscopic grade from aldrich.

2.2 Physical measurements

^{1}H NMR (400 MHz) and ^{13}C NMR (100 MHz) spectra were recorded on a Brucker Avance 400 spectrometer at room temperature using deuterated dimethyl sulphoxide (DMSO-d^{6}) solvent. IR spectra were recorded on a FT-IR ABB Bomen MB-3000 spectrophotometer. The melting points were determined on the thermocal10 melting point apparatus (Analab Scientific PVT.LTD, India) in open capillaries. Electronic spectra were recorded with UV-160A UV-Vis spectrophotometer, Shimadzu, Kyoto (Japan). Conductance measurements were carried out using conductivity meter model number E-660A. Model Euro Vector EA 3000 and Perkin Elmer 240 elemental analyzer were used for C, H, N- elemental analysis of ligand and complexes, respectively. Electron Spray ionization (ESI) mass spectra were obtained using thermo scientific mass spectrometer (USA). The structures were optimized by quantum mechanics methods. Optimization was performed using the Becke's three parameter hybrid exchange functional (B3) and the Lee–Yang–Parr correlation functional (LYP) (B3LYP) with the Gaussian 09 program package[20]. Calculations were done using

an Intel CORE i3, 2.40 GHz based machine running MS Windows 8.1, 32 bit, x64 based processor as the operating system.

2.3 Synthesis of substituted hydrazinyl pyridine based ligands (L^1-L^6)

A solution of substituted aldehyde (2a-2f, 1 mmol) was stirred in methanol at room temperature with 2- hydrazinyl pyridine (1a, 1 mmol) in the presence of the catalytic amount of acetic acid. The reaction was completed after 1 h, which was confirmed by TLC. The white precipitates of the desired product were obtained, which were filtered. The purity of product was checked on the TLC plate in ethyl acetate: n-hexane system (30:70).

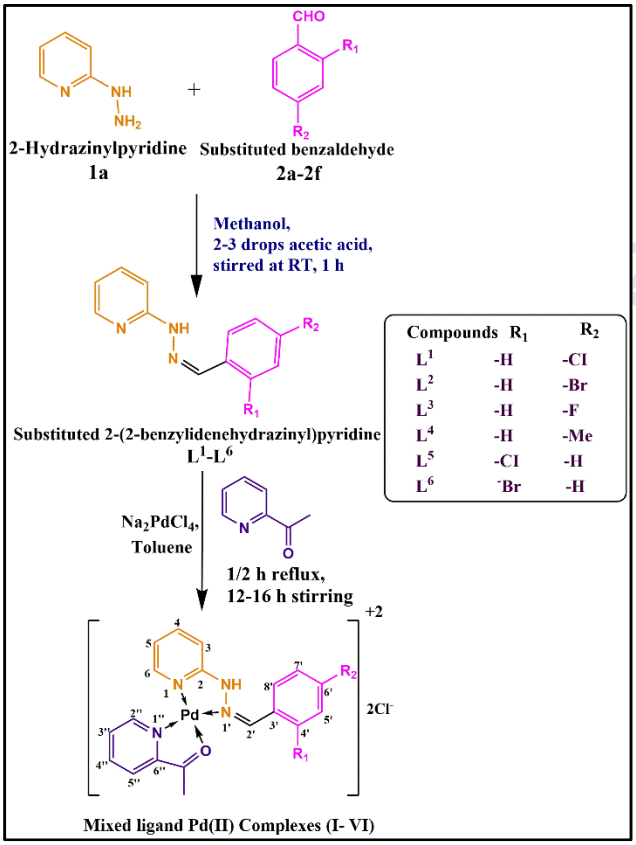

Scheme 1. Reaction scheme for mixed-ligands palladium complexes (I-VI).

2.3.1 2-(2-(4-Chlorobenzylidene)hydrazinyl)pyridine (L^1)

This ligand (L^1) was prepared using 2- hydrazinyl pyridine (1a) (0.01 mmol) and 4- chloro benzaldehyde (2a) (0.01 mmol). Color: White, Yield: 81%, mol. wt.: 231.68 g/mol, m.p.: 275 - 278 °C, Anal. Calc. (%) for $C_{12}H_{10}CIN_3$: C, 62.21; H, 4.35; N, 18.14; Found (%): C, 62.03; H, 4.54; N, 17.99. ^{1}H NMR (400 MHz, DMSO-d_6) δ/ppm: 8.92 (1H, s, -N-H), 8.17-8.16 (1H, m, H_6), 7.74 (1H, s, $H_{2'}$), 7.67-7.61 (3H, m, $H_{4',8',4}$), 7.40- 7.36 (3H, m, $H_{5',7',5}$), 6.84-6.80 (1H, m, H_3). ^{13}C NMR (100 MHz, DMSO-d_6) δ/ppm: 156. 6 (C_2, C_{qut}), 147.4

($C_{2'}$, -CH), 138.2 (C_6, -CH), 137.7 ($C_{4',8'}$, -CH), 134.5 ($C_{6'}$, $C_{quat.}$), 133.5 ($C_{3'}$, C_{quat}), 128.9 ($C_{5',7'}$, -CH), 127.5 (C_4, -CH), 116.0 (C_5, -CH), 107.6 (C_3, -CH). [Total signal observed = 10: signal of C_{qut} = 3, signal of -CH = 7)].

2.3.2 2-(2-(4-Bromobenzylidene)hydrazinyl)pyridine (L^2)

This ligand (L^2) was prepared using 2- hydrazinyl pyridine (1a) (0.01 mmol) and 4- bromo benzaldehyde (2b) (0.01 mmol). Color: White, Yield: 83%, mol. wt.: 276.14 g/mol, m.p.: 268 – 271 °C, Anal. Calc. (%) for $C_{12}H_{10}BrN_3$: C, 52.20; H, 3.65; N, 15.22; Found (%): C, 52.16; H, 3.54; N, 15.39. ^{1}H NMR (400 MHz, DMSO-d_6) δ/ppm: 8.62 (1H, s, -N-H), 8.16 (1H, d, J = 4.4 Hz, H_6), 7.72 (1H, s, $H_{2'}$), 7.67-7.62 (2H, m, $H_{4',8'}$), 7.58-7.52 (3H, m, $H_{4,5',7'}$), 7.38 (1H, d, J= 8.4 Hz, H_3), 6.82 (1H, dd, J_1 = 5.2, J_2 = 7.2 Hz, H_5). ^{13}C NMR (100 MHz, DMSO-d_6) δ/ppm: 157.4 (C_2, C_{qut}), 147.6 ($C_{2'}$, -CH), 142.4 ($C_{6'}$, -C_{quat}), 138.2 (C_6, -CH), 137.7 (C_4, -CH), 131.8 ($C_{5',7'}$, -CH), 127.8 ($C_{4',8'}$, -CH), 122.6 ($C_{3'}$, C_{quat}), 116.1 (C_5, -CH), 107.6 (C_3, -CH). [Total signal observed = 10: signal of C_{qut} = 3, signal of -CH = 7)].

2.3.3 2-(2-(4-Flourobenzylidene)hydrazinyl)pyridine (L^3)

This ligand (L^3) was prepared using 2- hydrazinyl pyridine (1a) (0.01 mmol) and 4- flouro benzaldehyde (2c) (0.01 mmol). Color: White, Yield: 86%, mol. wt.: 215.23 g/mol, m.p.: 249 – 251 °C, Chemical formula: $C_{12}H_{10}FN_3$. ^{1}H NMR (400 MHz, DMSO-d_6) δ/ppm: 8.69 (1H, s, -N-H), 8.16 (1H, s, $H_{2'}$), 7.77 (2H, d, J = 12.0 Hz, $H_{4',8'}$), 7.67-7.62 (2H, m, $H_{4,6}$), 7.38 (2H, d, J = 8.0 Hz, $H_{5',7'}$), 7.12-7.07 (1H, m, H_3), 6.79 (1H, dd, J_1 = 3.2, J_2 = 8.0 Hz, H_5). ^{13}C NMR (100 MHz, DMSO-d_6) δ/ppm: 154.4 (C_2, C_{qut}), 147.6 (C_6, -CH), 138.1 ($C_{2'}$, -CH), 137.8 (C_4, -CH), 134.2 ($C_{6'}$, $C_{quat.}$), 128.1 ($C_{4',8'}$ -CH), 123.4 ($C_{3'}$, $C_{quat.}$), 115.9 (C_5, -CH), 115.6 ($C_{5',7'}$, -CH), 107.5 (C_3, -CH). [Total signal observed = 10: signal of C_{qut} = 3, signal of -CH = 7)].

2.3.4 2-(2-(4-Mehtylbenzylidene)hydrazinyl)pyridine (L^4)

This ligand (L^4) was prepared using 2- hydrazinyl pyridine (1a) (0.01 mmol) and 4- methyl benzaldehyde (2d) (0.01 mmol). Color: White, Yield: 80%, mol. wt.: 211.27 g/mol, m.p.: 243 – 245 °C, Anal. Calc. (%) for $C_{13}H_{13}N_3$: C, 73.91; H, 6.20; N, 19.89; Found (%): C, 74.06; H, 6.54; N, 19.99. ^{1}H NMR (400 MHz, DMSO-d_6) δ/ppm: 8.60 (1H, s, -N-H), 8.17-8.15 (1H, m, H_6), 7.76 (1H, s, $H_{2'}$), 7.65-7.58 (3H, m, $H_{4',8',4}$), 7.39 (1H, d, J = 8.4 Hz, H_3), 7.22 (2H, d, J= 8.0 Hz, $H_{5',7'}$), 6.81-6.79 (1H, m, H_5), 2.40 (3H, s, -CH_3). ^{13}C NMR (100 MHz, DMSO-d_6) δ/ppm: 156.8 (C_2, C_{qut}), 147.6 (C_6, -CH), 139.3 ($C_{2'}$, -CH), 139.0 ($C_{6'}$, $C_{quat.}$), 138.1 (C_4, -CH), 132.2 ($C_{3'}$, C_{quat}), 129.4 ($C_{5',7'}$, -CH), 126.4 ($C_{4',8'}$, -CH), 115.6

($C_{5,}$ -CH), 107.5 ($C_{3,}$ -CH), 21.4 (-$CH_{3,}$ -Methyl). [Total signal observed = 11: signal of C_{qut} = 3, signal of –CH and CH_3 = 8)].

2.3.5 2-(2-(2-Chlorobenzylidene)hydrazinyl)pyridine (L^5)

This ligand (L^5) was prepared using 2- hydrazinyl pyridine (1a) (0.01 mmol) and 2- chloro benzaldehyde (2e) (0.01 mmol). Color: White, Yield: 89%, mol. wt.: 231.68 g/mol, m.p.: 269 – 272 °C, Anal. Calc. (%) for $C_{12}H_{10}ClN_3$: C, 62.21; H, 4.35; N, 18.14; Found (%): C, 62.16; H, 4.54; N, 18.09. ^{1}H NMR (400 MHz, DMSO-d_6) δ/ppm: 9.56 (1H, s, -N-H), 8.23 (1H, s, $H_{2'}$), 8.09 (2H, dd, J_1 = 1.6, J_2 = 7.6, $H_{6, 8'}$), 7.67-7.63 (1H, m, $H_{5'}$), 7.43-7.37 (2H, m, $H_{6',7'}$), 7.31 (1H, t, J = 7.2 Hz, H_4), 7.26 (1H, dd, J_1 = 5.6, J_2 = 7.6 Hz, H_5), 6.84 (1H, t, J = 5.6 Hz, H_3). ^{13}C NMR (100 MHz, DMSO-d_6) δ/ppm: 157.7 ($C_{2,}$ C_{qut}), 147.6 ($C_{2',}$ -CH), 142.8 ($C_{3',}$ $C_{quat.}$), 138.1 ($C_{6,}$ -CH.), 135.4 (C_4, -CH.), 130.0 ($C_{5',}$ -CH), 129.6 ($C_{6',}$ -CH.), 126.9 ($C_{7',}$ -CH), 126.6 ($C_{8',}$ -CH), 120.2 ($C_{4',}$ -C_{quat}), 116.1 ($C_{5,}$ -CH), 107.6 (C_3, -CH). [Total signal observed = 12: signal of C_{qut} = 3, signal of -CH = 9)].

S

2.3.6 2-(2-(2-Bromobenzylidene)hydrazinyl)pyridine (L^6)

This ligand (L^6) was prepared 2- hydrazinyl pyridine (1a) (0.01 mmol) and 2- bromo benzaldehyde (2f) (0.01 mmol). Color: White, Yield: 87%, mol. wt.: 276.14 g/mol, m.p.: 254 – 257 °C, Anal. Calc. (%) for $C_{12}H_{10}BrN_3$: C, 52.20; H, 3.65; N, 15.22; Found (%): C, 52.10; H, 3.59; N, 15.49. ^{1}H NMR (400 MHz, DMSO-d_6) δ/ppm: 9.14 (1H, s, -N-H), 8.22 (1H, dd, J_1 = 0.8, J_2 = 4.8 Hz, H_4), 8.18 (1H, s, $H_{2'}$), 7.67- 7.63 (1H, m, H_5), 7.61-7.56 (1H, m, H_6), 7.42-7.32 (4H, m, $H_{5',6',7',8'}$), 7.21- 7.18 (1H, m, H_3). ^{13}C NMR (100 MHz, DMSO-d_6) δ/ppm: 153.6 ($C_{2,}$ C_{qut}), 147.6 ($C_{2',}$ -CH), 144.0 ($C_{3',}$ $C_{quat.}$), 138.2 ($C_{6,}$ -CH.), 137.8 (C_4, -CH.), 133.1 ($C_{6',}$ -CH), 129.9 ($C_{5',}$ -CH.), 127.5 ($C_{8',}$ -CH), 127.1 ($C_{7',}$ -CH), 123.1 ($C_{4',}$ C_{quat}), 116.1 ($C_{5,}$ -CH), 107.6 (C_3, -CH). [Total signal observed = 12: signal of C_{qut} = 3, signal of -CH = 9].

2.4 General method for synthesis of mixed-ligands palladium(II) complexes (I-VI)

The methanolic solution of substituted hydrazinyl pyridine based Schiff base (L^1-L^6) (0.0001 M) was drop wise added to a methanolic solution of Na_2PdCl_4 (0.0001 M). The mixture was warmed for 10 minutes, followed by the addition of 2-acetylpyridine (0.0001 M). The resulted solution was refluxed at 60 °C. After 30 min, the stirring was carried out at room temperature for 12-16 h. The obtained product was washed with diethyl ether and hexane and dried to get yellow powder.

2.4.1 Palladium(II) complex (I) [Pd(L^1)2-acpy]Cl_2

This complex was prepared using ligand (L^1) (0.01 mmol), 2- acetyl pyridine (0.01 mmol) and Na_2PdCl_4 salt (0.01 mmol) as described in general process. Color: yellow, Yield: 86%, mol. wt.: 530.24 g/mol, m.p.: > 300 °C Anal. Calc. (%) for $C_{19}H_{17}Cl_3N_4OPd$: C, 43.05; H, 3.23; N, 10.57; Pd, 20.07; Found (%): C, 43.50; H, 3.56; N, 10.23; Pd, 20.78. ^{1}H NMR (400 MHz, DMSO-d_6) δ/ppm: 12.44 (1H, s, -N-H), 8.17 (1H, d, J = 5.6 Hz, $H_{2''}$), 8.01 (1H, s, $H_{2'}$), 7.83 (2H, t, J = 8.0 Hz, $H_{3'',4''}$), 7.93 (2H, d, J =5.2 Hz, $H_{3,6}$), 7.47 (2H, d, J = 4.8 Hz, $H_{5',7'}$), 7.26-7.23 (2H, m, $H_{4,5}$), 7.17 (1H, d, J = 6.8 Hz, $H_{5''}$), 6.97 (2H, t, $H_{4',8'}$), 3.44 (3H, s, -Methyl). ^{13}C NMR (100 MHz, DMSO-d_6) δ/ppm: 173.2 (>C=O, C_{quat}), 157.3 ($C_{6''}$, C_{qut}), 155.4 (C_2, C_{quat}), 147.4 ($C_{2'}$, -CH), 146.0 ($C_{2'',4''}$, -CH), 141.3 (C_4, -CH), 138.4 ($C_{3'}$, C_{quat}), 133.2 (C_6, -CH), 130.0 ($C_{5',7'}$, -CH), 127.5 ($C_{4',8'}$, -CH), 124.9 ($C_{5''}$, -CH), 122.1 ($C_{6'}$, C_{quat}), 116.8 ($C_{3''}$, -CH), 114.4 (C_5, -CH), 108.5 (C_3, -CH), 33.5 (Methyl, -CH_3). [Total signal observed = 16: signal of C_{qut} = 5, signal of -CH and CH_3= 11)].

2.4.2 Palladium(II) complex (II) [Pd(L^2)2-acpy]Cl_2

This complex was prepared using ligand (L^2) (0.01 mmol), 2- acetyl pyridine (0.01 mmol) and Na_2PdCl_4 salt (0.01 mmol) as described in general process. Color: yellow, Yield: 82%, mol. wt.: 574.96 g/mol, m.p.: > 300 °C Anal. Calc. (%) for $C_{19}H_{17}BrCl_2N_4OPd$: C, 39.72; H, 2.98; N, 9.57; Pd, 18.52; Found (%): C, 39.06; H, 2.52; N, 9.99; Pd, 18.43. ^{1}H NMR (400 MHz, DMSO-d_6) δ/ppm: 12.60 (1H, s, -N-H), 7.91 (1H, d, J = 4.4 Hz, $H_{2''}$), 7.82 (2H, t, J = 8.0 Hz, $H_{3'',4''}$), 7.74 (1H, s, $H_{2'}$), 7.29 (2H, d, J = 1.6 Hz, $H_{3,6}$), 7.16 (2H, dd, J_1 = 1.6, J_2 = 8.0 Hz, $H_{5',7'}$), 7.11 (1H, d, J = 8.0 Hz, $H_{5''}$), 6.96 (2H, t, J = 6.0 Hz, $H_{4,5}$), 6.87 (2H, d, J = 8.4 Hz, $H_{4',8'}$), 3.45 (3H, s, -Methyl). ^{13}C NMR (100 MHz, DMSO-d_6) δ/ppm: 175.7 (>C=O, C_{quat}), 157.9 ($C_{6''}$, C_{qut}), 155.8 (C_2, C_{quat}), 150.4 ($C_{2'}$, -CH), 149.6 ($C_{3'}$, $C_{quat.}$), 146.0 ($C_{2'',4''}$, -CH), 141.2 (C_6, -CH), 136.2 ($C_{5',7'}$, -CH), 131.8 ($C_{4',8'}$, -CH), 128.0 ($C_{3''}$, -CH), 127.2 ($C_{5''}$, -CH), 121.7 ($C_{6'}$, C_{quat}), 120.0 (C_4, -CH), 116.6 (C_5, -CH), 108.4 (C_3, -CH), 35.2 (Methyl, -CH_3). [Total signal observed = 16: signal of C_{qut} = 5, signal of -CH and CH_3= 11)].

2.4.3 Palladium(II) complex (III) [Pd(L^3)2-acpy]Cl_2

This complex was prepared using ligand (L^3) (0.01 mmol), 2- acetyl pyridine (0.01 mmol) and Na_2PdCl_4 salt (0.01 mmol) as described in general process. Color: yellow, Yield: 85%, mol. Wt.: 513.69 g/mol, m.p.: > 300 °C, Anal. Calc. (%) for $C_{19}H_{17}Cl_2FN_4OPd$. Pd, 20.72; Found (%): Pd, 20.86. ^{1}H NMR (400 MHz, DMSO-d_6) δ/ppm: 12.42 (1H, s, -N-H), 8.00 (1H, d, J = 4.4 Hz, $H_{2''}$), 7.92 (1H, d, J = 5.2 Hz, H_6), 7.81 (2H, t, J = 7.6 Hz, $H_{3'',4''}$), 7.74 (1H, s, $H_{2'}$), 7.45 (2H, t, J = 8.8 Hz, $H_{4,5}$), 7.24 (1H, d, J = 6.0 Hz, H_3), 6.96- 6.90 (4H, m, $H_{4',5',7',8'}$), 6.76 (1H, d, J = 6.0 Hz, $H_{5''}$), 3.74 (3H, s, -Methyl). ^{13}C NMR (100 MHz, DMSO-d_6) δ/ppm: 178.4 (>C=O, C_{quat}), 158.4 ($C_{6''}$, C_{quat}), 156.8 (C_2, C_{quat}), 150.3 ($C_{2'',4''}$ -CH), 146.0 ($C_{2'}$, -CH), 141.1 (C_6, -CH), 139.3 ($C_{3'}$, C_{quat}), 132.8 ($C_{4',8'}$, -CH), 128.1 ($C_{6'}$, C_{quat}), 121.1 (C_4, -CH), 120.9 ($C_{5''}$, -CH), 116.3 ($C_{5',7'}$, -CH), 110.9 ($C_{3''}$, -CH), 110.7 (C_5, -CH), 108.4 (C_3, -CH), 34.9 (Methyl, -CH_3). [Total signal observed = 16: signal of C_{quat} = 5, signal of -CH and CH_3= 11)].

2.4.4 Palladium(II) complex (IV) [Pd(L^4)2-acpy]Cl_2

This complex was prepared using ligand (L^4) (0.01 mmol), 2- acetyl pyridine (0.01 mmol) and Na_2PdCl_4 salt (0.01 mmol) as described in general process. Color: yellow, Yield: 89%, mol. wt.: 509.73 g/mol, m.p.: > 300 °C, Anal. Calc. (%) for $C_{20}H_{20}Cl_2N_4OPd$: C, 47.13; H, 3.96; N, 10.99; Pd, 20.88; Found (%): C, 47.16; H, 3.54; N, 10.19; Pd, 20.93. ^{1}H NMR (400 MHz, DMSO-d_6) δ/ppm: 12.34 (1H, s, -N-H), 7.90 (2H, d, J = 5.6 Hz, $H_{2'',5''}$), 7.78 (2H, t, J = 8.0 Hz, $H_{3'',4''}$), 7.67 (1H, s, $H_{2'}$), 7.42 (1H, d, J = 8.4 Hz, H_6), 7.04 (2H, t, J = 6.4 Hz, $H_{4,5}$), 6.93 (2H, d, J = 6.4 Hz, $H_{4',8'}$), 6.84 (2H, d, J = 8.8 Hz, $H_{5',7'}$), 6.73 (1H, d, J = 7.6 Hz, H_3), 3.52 (3H, s, -Methyl(acetyl moiety)), 2.18 (3H, s, Methyl). ^{13}C NMR (100 MHz, DMSO-d_6) δ/ppm: 177.0 (>C=O, C_{quat}), 157.8 ($C_{6''}$, C_{qut}), 155.3 (C_2, C_{quat}), 151.0 ($C_{2'}$, -CH), 145.8 ($C_{3'}$, $C_{quat.}$), 140.8 ($C_{2',4''}$, -CH), 138.0 (C_4, -CH), 135.4 ($C_{6'}$, -$C_{quat.}$), 130.1 (C_6, -CH), 129.7 ($C_{5',7'}$, -CH), 126.2 ($C_{4',8'}$, -CH), 124.8 ($C_{3''}$, -CH), 120.0 ($C_{5''}$, -CH), 116.2 (C_5, -CH), 108.2 (C_3, -CH), 33.2 (Methyl (acetyl moiety), -CH_3), 21.5 (Methyl, -CH_3). [Total signal observed = 17: signal of C_{qut} = 5, signal of -CH and CH_3= 12)].

2.4.5 Palladium(II) complex (V) [Pd(L^5)2-acpy]Cl_2

This complex was prepared using ligand (L^5) (0.01 mmol), 2- acetyl pyridine (0.01 mmol) and Na_2PdCl_4 salt (0.01 mmol) as described in general process. Color: yellow, Yield: 86%, mol. wt.: 530.14 g/mol, m.p.: > 300 °C, Anal. Calc. (%) for $C_{19}H_{17}Cl_3N_4OPd$: C, 43.05; H, 3.25; N, 10.57; Pd, 20.07; Found (%): C, 43.32; H, 3.84; N, 10.89; Pd, 20.83. ^{1}H NMR (400 MHz, DMSO-d_6) δ/ppm: 12.54 (1H, s, -N-H), 8.17 (1H, d, J = 5.2 Hz, $H_{2''}$), 7.93

(2H, d, J = 4.8 Hz, $H_{3,6}$), 7.83 (1H, s, $H_{2'}$), 7.76 (2H, t, J = 8.0 Hz, $H_{3'',4''}$), 7.47 (2H, d, J = 3.2 Hz, $H_{5',8'}$), 7.28 (2H, t, $H_{4,5}$), 7.17 (1H, d, J = 6.0 Hz, $H_{5''}$), 6.97 (2H, t, J = 6.0 Hz, $H_{6',7'}$), 3.43 (3H, s, -Methyl). ^{13}C NMR (100 MHz, DMSO-d_6) δ/ppm: 176.4 (>C=O, C_{quat}), 156.3 ($C_{6''}$, C_{qut}), 154.5 (C_2, C_{quat}), 147.4 ($C_{2'}$, -CH), 146.0 ($C_{2'',4''}$, -CH), 141.3 (C_4, -CH), 139.1 ($C_{3'}$, C_{quat}), 133.2 (C_6, -CH), 130.0 ($C_{5',6',8'}$, -CH), 127.5 ($C_{7'}$, -CH), 124.9 ($C_{3'',5''}$, -CH), 122.3 ($C_{4'}$, C_{quat}), 116.9 (C_5, -CH), 108.5 (C_3, -CH), 33.8 (Methyl, -CH_3). [Total signal observed = 15: signal of C_{qut} = 5, signal of -CH and CH_3= 10)].

2.4.6 Palladium(II) complex (VI) [Pd(L^6)2-acpy]Cl_2

This complex was prepared using ligand (L^6) (0.01 mmol), 2- acetyl pyridine (0.01 mmol) and Na_2PdCl_4 salt (0.01 mmol) as described in general process. Color: yellow, Yield: 86%, mol. wt.: 574.60 g/mol, m.p.: > 300 °C, Anal. Calc. (%) for $C_{19}H_{17}BrCl_2N_4OPd$: C, 39.72; H, 2.98; N, 9.75; Pd, 18.52; Found (%): C, 39.07; H, 2.13; N, 9.97; Pd, 18.78. ^{1}H NMR (400 MHz, DMSO-d_6) δ/ppm: 12.54 (1H, s, -N-H), 7.93 (1H, d, J = 5.2 Hz, $H_{2''}$), 7.84 (2H, t, J = 8.0 Hz, $H_{3'',4''}$), 7.79 (1H, s, $H_{2'}$), 7.22 (2H, d, J = 7.2 Hz, $H_{3,6}$), 7.11 (2H, d, J = 8.0 Hz, $H_{5',8'}$), 6.99 (2H, t, J = 6.4 Hz, $H_{4,5}$), 6.91 (1H, d, J = 8.4 Hz, $H_{5''}$), 6.84 (2H, t, J = 8.0 Hz, $H_{6',7'}$), 3.52 (3H, s, -Methyl). ^{13}C NMR (100 MHz, DMSO-d_6) δ/ppm: 176.6 (>C=O, C_{quat}), 158.5 ($C_{6''}$, C_{qut}), 156.8 (C_2, C_{quat}), 151.3 ($C_{2'}$, -CH), 150.1 ($C_{3'}$, C_{quat}), 146.2 ($C_{2'',4''}$, -CH), 142.1 (C_4, -CH), 138.5 (C_6, -CH), 133.8 ($C_{5',8'}$, -CH), 128.0 ($C_{6',7'}$, -CH), 127.8 ($C_{5''}$, -CH), 122.5 ($C_{4'}$, C_{quat}), 121.4 ($C_{3''}$, -CH), 113.2 (C_5, -CH), 105.2 (C_3, -CH), 34.4 (Methyl, -CH_3). [Total signal observed = 16: signal of C_{qut} = 5, signal of -CH and CH_3= 11)].

2.5 Biological screening of compound

2.5.1 Antibacterial activity by broth dilution method

The minimum inhibitory concentration (MIC) is defined as the lowest concentration of bacterial agents that prevent the growth of bacteria (bacteriostatic). The *in vitro* antibacterial activity of hydrazinyl pyridine based Schiff bases (L^1-L^6) and their metal complexes (I-VI) were carried out against the two Gram(+ve) and three Gram(-ve) bacteria using broth dilution method. All the bacteria were grown in 5 mL sterile nutrient or Luria broth solution and incubated overnight at 37 °C. Different concentrations of the compounds were injected with cultured bacteria. The next day, effects were checked to determine at what level the MIC value is established [21, 22].

2.5.2 Evaluation of *in vitro* cytotoxicity

Brine shrimp lethality bioassay is a simple, reliable and convenient method used for the evaluation of bioactivity of compounds and it extends for preliminary assessment of toxicity. The cytotoxicity was reported in terms of lethal concentration (LC_{50}). Commercial sea salt was used for the preparation of artificial sea water (5%) for hatching brine shrimp eggs. The incubation at 26-30 °C for 48 h results into free nauplii from eggshells, which were collected using a light source and used for the screening. Ten active shrimps were added in each test tube and volume was adjusted to 2500 µL per test tube to obtain different concentrations. The surviving shrimp were counted after 24 h and lethal concentration LC_{50} was assessed and percentage mortality (% M) of nauplii was plotted against the log of the concentration of compounds [23, 24].

2.5.3 Cellular level cytotoxicity against *S. pombe* cells

The cellular level bioassay was carried out using *S. pombe* cells. *S. pombe* is harmless, rapidly growing eukaryotes that are popular as model systems to understand basic biological processes. *In vivo* cytotoxicity experiment was performed according to previously published literature [25].

2.5.4 Cell line study

The human colorectal cancer cell line HCT-116 was purchased from the national centre for cell science (NCCS), Pune, Maharashtra, India. The cell cultures were maintained under controlled conditions in a humidified atmosphere with 5% CO_2 at 37°C in culture flasks. The cells were grown in complete RPMI-1640 medium supplemented with 10% FBS and 1% PSN, an antibiotics mixture (Life technologies, USA). Exponentially growing HCT-116 cells were exposed to compounds and vehicle (1% DMSO) for 24 h. therefore, the cells were washed with DPBS and incubated with MTT solution for 4 h in dark at 37°C. After incubation, the MTT was removed and DMSO was added to each well. The absorbance was taken at 570 nm with a reference wavelength of 650 nm by using a multimode microplate reader.

2.6 DNA interaction studies

2.6.1 Electronic absorption spectra

The interaction of complexes with HS-DNA was investigated using UV-visible spectroscopy. The stock solutions of metal complexes were prepared using DMSO and diluted with phosphate buffer (pH = 7.2) to the required concentration for whole experiments. Absorption titration experiments were performed by maintaining a constant concentration of the complexes and HS-DNA concentration (0-100 µM) with varying volume (0-500 µL). The UV-visible spectra of the complexes in the presence of HS-DNA were scanned against phosphate buffer solution in the range from 200 to 800 nm wavelength [26].

2.6.2 Hydrodynamic volume measurement

Viscosity measurement was used for further clarification of the DNA binding interaction of the metal complexes. In this experiment, the HS-DNA solution (200 µM) was mixed with an increasing amount of complexes and the relative viscosity of these solutions was measured using Ubbelohde viscometer at 25.0 ± 0.5 °C. The data were obtained as $(\eta/\eta_0)^{1/3}$ vs. [complex/HS-DNA], where η_0 and η are the viscosity of HS-DNA in the absence and presence of the metal complexes, respectively. Viscosity values were calculated from the observed flow time of DNA containing solution (t) corrected for buffer alone (t_0), $\eta \alpha (t-t_0)$ [27, 28].

2.6.3 EB-displacement study

Fluorescence emission studies were carried out according to the previously reported literature [29].

2.6.4 Molecular docking study

The docking study of Pd(II) complex with DNA was performed using the Hex 8.0 software. The binding position and bound conformation of the macromolecule with complexes and approximate calculation of their interactions were analyzed with the hex software. Docking needs data bank for the search target with proper PDB format. These tools provide the information about the interaction between DNA and complexes. DNA sequence $d(ACCGACGTCGGT)_2$ (1BNA) of the structure was used for interaction study and obtained from the protein data bank [30, 31].

2.6.5 DNA cleavage via agarose gel electrophoresis

Agarose gel electrophoresis experiment was carried out to monitor the cleavage of DNA by synthesized complexes. The experimental procedure was performed according to the reported procedure [25].

2.7 Protein binding study

The Serum albumin(SA)-binding study was performed by UV-visible electronic absorption titration using BSA in phosphate buffer (Na_2HPO_4/NaH_2PO_4, pH 7.2) solution. In this study, titration of BSA with mixed-ligand Pd(II) complexes was carried out. The absorption titration spectra of BSA (15 µM) and the solution of mixed-ligand Pd(II) complexes at 0, 8, 16, 24, 32, 40 µM concentration were measured in the range of 200-800 nm. In each fraction, after the addition of metal complexes, solution was incubated for 7 min., and the absorption spectra were overlaid [32].

3. Result and discussion

3.1 ^{1}H NMR spectra

The ^{1}H NMR spectra of the Schiff base ligands (L^1-L^6) and their mixed-ligand palladium(II) complexes (I-VI) were obtained in solvent DMSO-d_6 as shown in supplementary material 1 and their physiochemical data of the compounds are summarized in the experimental section. In the aromatic region, ten protons are observed for ligands (L^1-L^6) and fourteen protons are observed for palladium(II) complexes (I-VI). In Schiff base ligands (L^1-L^6), all aromatic protons appear in the range of 8.23 – 6.79 δ ppm while for Pd(II) complexes, appeared in the range of 8.17 – 6.73 δ ppm. The NMR signal for imine (-N-H) group of ligands and complexes are appeared at around 9.56 – 8.60 δ ppm and 12.60 – 12.34 δ ppm, respectively. The signal shift in the ^{1}H NMR spectra suggests the involvement of pyridine ring nitrogen as a coordinating atom.

3.2 ^{13}C NMR spectra

The ^{13}C NMR spectra of the synthesized Schiff base ligands (L^1-L^6) and mixed-ligand palladium(II) complexes (I-VI) are shown in supplementary material 2 and their physicochemical data are represented in the experimental section. The peak of the methyl group in the ligand (L^4) and complex (IV) is observed at 21.43 ppm and 21.47 ppm, respectively. The heteroleptic Pd(II) complexes (I-VI) containing 2-acetylpyridine

bidentate ligands having >C=O peak appeared in the range of 173.0-177.0 ppm. In ligands, the peak of the C_2 and C_{quat} are observed in the range of 153.6-157.7 ppm. In complexes, the peaks of C_2, and C_{quat} are shifted to the downfield region at 156.3-158.4 ppm.

3.3 Mass spectra

The mass spectra and fragmentation pattern of hydrazinyl pyridine based ligands (L^1-L^6) are shown in supplementary material 3. The mass spectra of complex (I) shows a molecular ion peak $[M\text{-}2Cl]^+$ at 459.0 m/z and $[M\text{-}2Cl+2]^+$ at 461.3 m/z. The peak at 338.10 m/z is due to the loss of 2-acetyl pyridine moiety from the complex. The peak at 233.90 m/z is due to the loss of palladium metal ion. The ESI-MS spectrum and possible mass fragmentation pattern of complex (I) are shown in supplementary material 4.

3.4 Electronic spectra, magnetic behaviour, conductance measurement, and structure optimization

The electronic spectra of mixed-ligand Pd(II) complexes were recorded in DMSO. The electronic spectra of palladium(II) complexes show absorption peak at around 273-277 nm (MLCT) and 451-456 nm (d-d transition), which suggest square planar geometry of the complexes. The magnetic moment measurement of all the synthesized mixed-ligand Pd(II) complexes is found to be zero, which is comparable to theoretical spin only value of square planar complexes indicating diamagnetic nature and d^8-low spin, with dsp^2 hybridization. The observed molar conductance (25-40 Ω^{-1} cm^2 mol^{-1}) in 10^{-3} DMSO solution of the complexes is consistent with the electrolytic nature of the complexes and presence of two chlorine ion as a counter ion outside the coordination sphere [33, 34]. The structure of complexes was optimized by Gaussian 09 program software to get information about the relative position of ligands in the complexes. The optimized structures (Supplementary material 5) clearly show that the oxygen atom of the acetylpyridine ligand is trans to the pyridine group of the benzylidene hydrazinyl pyridine ligand. The pyridine rings of both the ligands are cis to each other.

3.5 Biological screening of compounds

3.5.1 *In vitro* antibacterial activity

The persistence and growth of antibiotic resistance in bacterial pathogens represent a public health concern. Antibacterial resistance may manipulate a biological cost, thereby

reducing the fitness of resistant strains, which can restrict the development of antibacterial resistant bacteria. Increased antibacterial resistance is the grounds of severe infections,

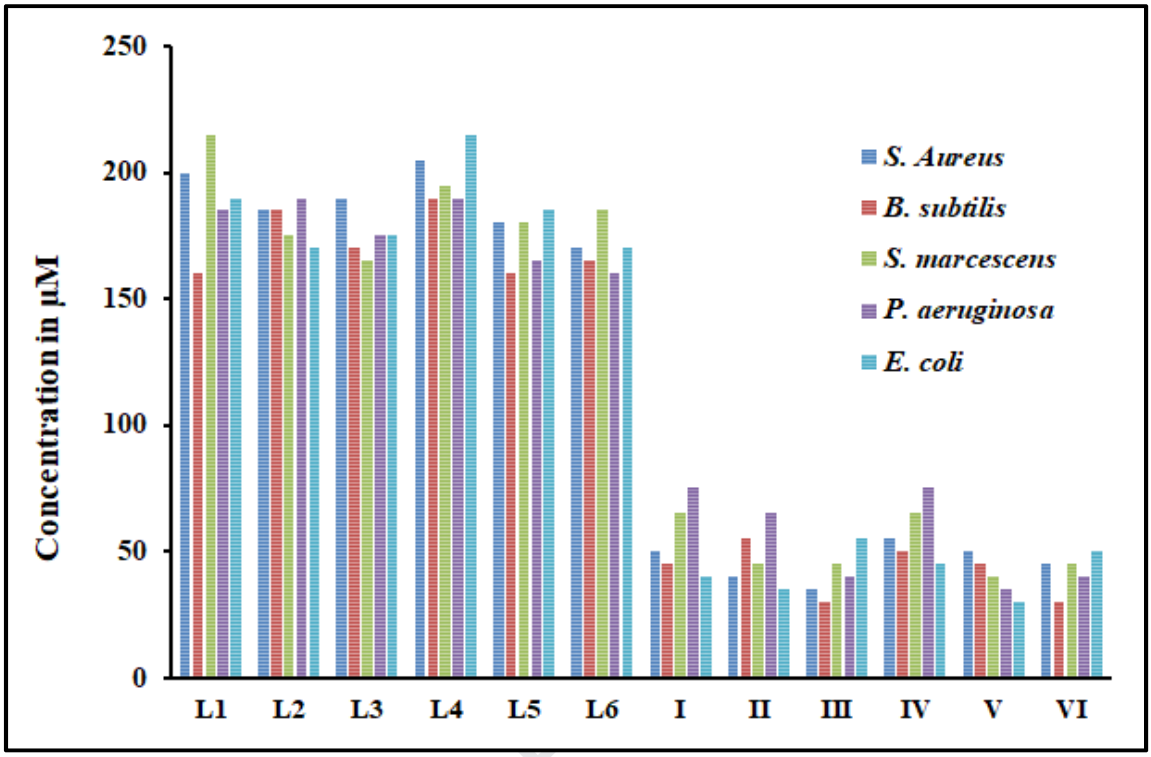

complications, and increased mortality. Some newly developed antibiotics have lost their efficacy against various bacterial infections within a few years after their debut. Metal coordination can alter the mechanism of drug activity, the antibacterial activity of the newly synthesized compound was tested against two Gram(+ve) negative and three Gram(-ve) bacterial strain using the broth dilution method**.** The results of the antibacterial study are represented in Fig. 1 and the data of the compounds are represented in supplementary material 6.

Figure 1. Effect of different concentrations of hydrazinyl pyridine based Schiff base (L^1-L^6) and mixed-ligand Pd(II) complexes on Gram(+ve) and Gram(-ve) bacteria.

MIC values of hydrazinyl based Schiff base and their corresponding mixed-ligand palladium(II) complexes are in the range of 150-215 µM and 30-85 µM respectively, which is comparable to previously reported palladium(II) complexes [35]. Complex VI has antibacterial activity against all tested bacterial strains with MIC value in the range of 30-45 µM. Compound VI has more potent activity with MIC value 30 µM against *B. subtilis*, 40 µM against *P. aeruginosa*. The complex V is most potent against *E. coli* with MIC value 30 µM. From this result, we can conclude that the metal ion upon chelation enhances the bacterial activity than the hydrazinyl based ligands. Tweedy's chelation theory predicts

that chelation reduces the polarity of the metal ions mainly because of partial sharing of its positive charge with donor group and possible electron delocalization over the entire ring. Therefore, increases in the lipophilic character of the chelates, favouring their permeation through the lipid layer of the bacterial membrane [36].

3.5.2 Brine shrimp lethality bioassay

In recent years, the brine shrimp lethality bioassay procedure of bioactive compounds has gained great attention to evaluate cytotoxicity as well as pharmacological activity of the compounds. The mortality rate of brine shrimp nauplii was found to increase with increase in the concentration of the compounds. The main advantages of brine shrimp lethality bioassay .are economical, inexpensive, short time generation than other cytotoxicity, and more reliable method. The LC_{50} data was calculated by the plot of percentage mortality of nauplii against the log of the concentration of the compounds, which is shown in Fig. 2, and data are represented in supplementary material 7. The LC_{50} values of the hydrazinyl Schiff base and their corresponding mixed ligand palladium(II) complexes are observed in the range of 9.24-14.12 µg/mL and 5.68-7.94 µg/mL, respectively, which are comparable with the previously reported Pd(II) complexes (8.31-16.80 µg/mL) [37]. From the data recorded, the palladium(II) complexes show good activity than ligands. The order of potency of compounds is cisplatin > V > VI > III > I > II > IV > L^3 > L^5 > L^6 > L^1 > L^2 > L^4 > transplatin.

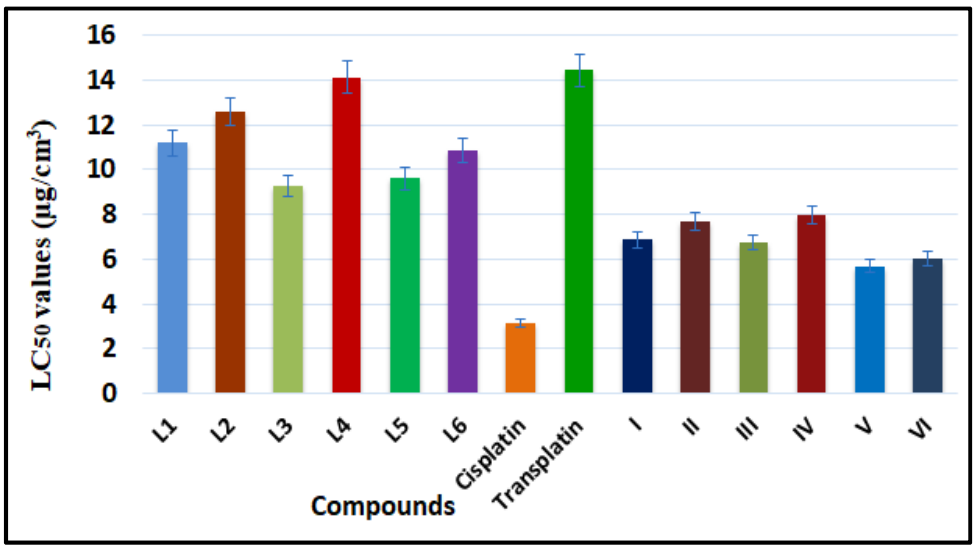

Figure 2. LC_{50} values of hydrazinyl based ligands and their corresponding mixed-ligand Pd(II) complexes, cisplatin and transplatin in µg/mL

3.5.3 *In vivo* cytotoxicity against *S. pombe* cells

The cell viability assay is designed to measure activities attributable to cellular maintenance and survival. The current most useful cytotoxicity biomarkers are constitutive conserved and relatively stable, high- abundance enzymes released into the culture medium following the loss of membrane integrity. The sixth model eukaryotic organism, *Schizosaccharomyces pombe*, was used in the study of the cellular response to DNA damage. The trypan blue dye used for the detection of *S. pombe* cells. Live cells or tissues with intact cell membranes are not colored. Since cells are very selective in the compounds that pass through the membrane in a viable cell trypan blue is not absorbed. Dead cells appear as a distinctive blue color under the microscope. Cellular level *in vivo* cytotoxicity against *S. pombe* cells was carried out using synthesized compounds, cisplatin, and transplatin. The toxicity was found to change with the different substituents present in the compounds. Complexes VI and V are found more toxic than other complexes against *S. pombe* cells. After 17 h treatment, *S. pombe* cells were killed due to the toxic nature of the compounds. Percentage viability graph and data of *in vivo* cellular level cytotoxicity against *S. pombe* are represented in Fig. 3 and supplementary material 8, respectively.

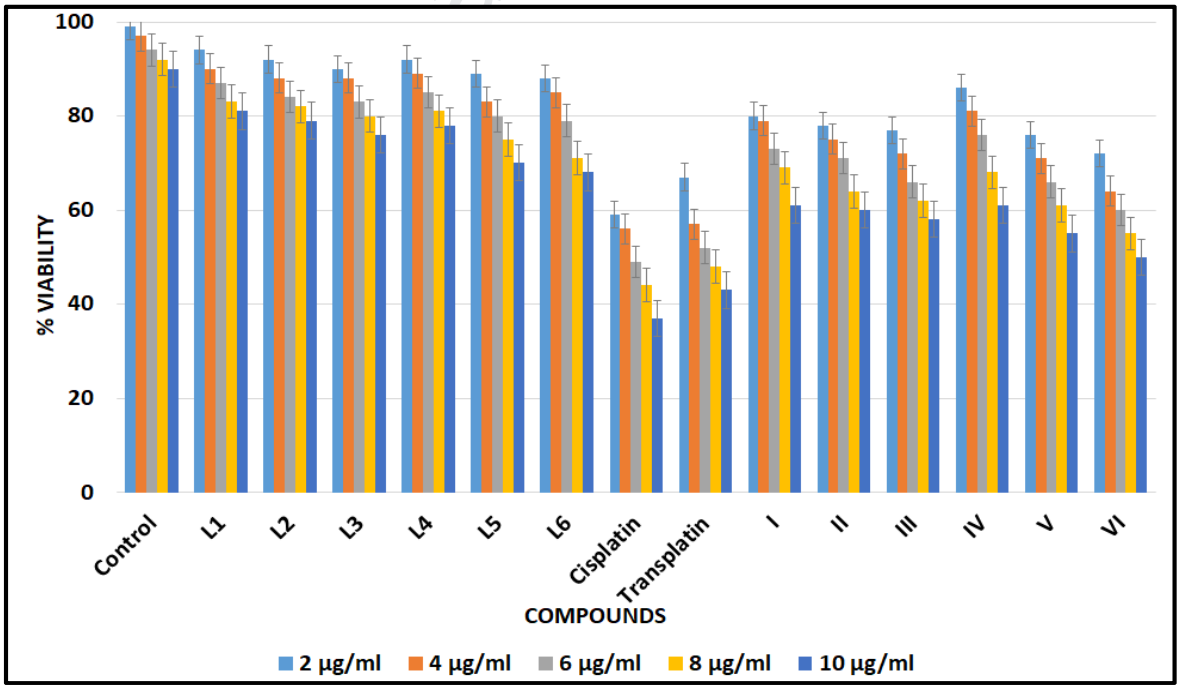

Figure 3. Cytotoxicity in terms of % cell viability of compounds at different concentrations.

3.5.4 Cell line study

For the investigation of potential synergetic cytotoxic effects, we evaluated cell anti-proliferation activity of Pd(II) complexes. Colorectal cancer is one of the most common malignancies worldwide [38] and hence the cytotoxicity of complexes I-VI was evaluated by MTT assay against human HCT-116 cancer cell line with cisplatin as positive controls. The IC_{50} value of the Pd(II) complexes (II, III, IV) exhibit some inhibitory effect on HCT-

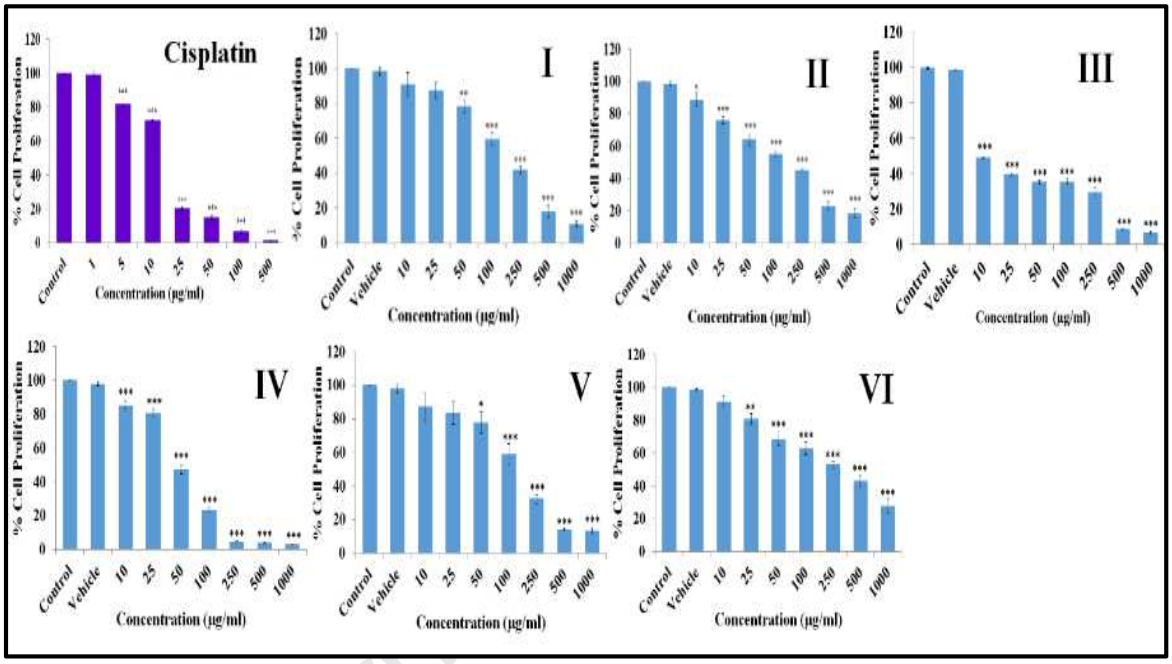

116 cancer cell line, while the palladium(II) complexes (I, V, VI) are found to be practically ineffective. Complexes (IV and V) are the most cytotoxic effect against human colorectal carcinoma HCT-116 cancer cell line compared to other complexes. The IC_{50} value of the palladium(II) complexes are found in increasing order of IV (51 µg/mL) > V (132 µg/mL) > II (138 µg/mL) > I (165 µg/mL) > VI (272 µg/mL) > III (283 µg/mL) > DMSO. Furthermore, the IC_{50} value of the mixed-ligand palladium(II) complex IV is lower than to standard drug carboplatin, but remaining complexes have higher IC_{50} value than standard drugs cisplatin (15 µg/mL), carboplatin (64.97 µg/mL) and oxaliplatin (25.74 µg/mL) [39]. The graph and values are represented in Fig. 4 and supplementary material 9, respectively.

Figure 4. Effect of synthesized mixed-ligand palladium(II) complexes on the proliferation of HCT-116 cells and determination of IC_{50} value of 10, 25, 50, 100, 250, 500, 1000 µg/mL Pd(II) complexes (I-VI), control (100% DMSO), and vehicle control (1% DMSO). Error bar represents standard deviation of three replicates.

3.5.5 General structure-activity relationship (SAR)

Different substituted benzyl rings on 2-hydrazino pyridine are widely affected the results of biological activities (Fig. 5). The complexes (I, II, IV) containing chloro (-CI), bromo (-

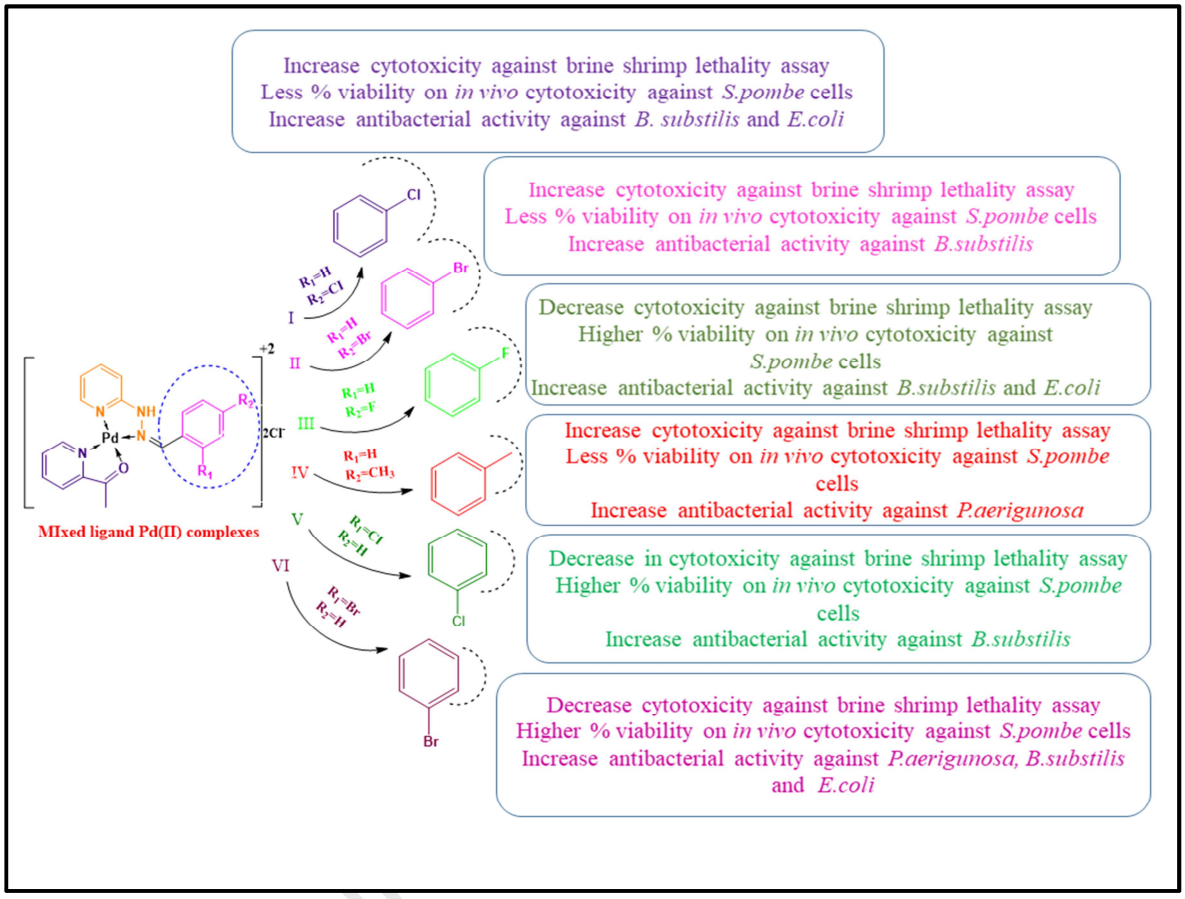

Br), and methyl (-CH_3) substituent at para position on benzyl ring increase the cytotoxicity in brine shrimp lethality bioassay. The para position having fluoro (complex III) and ortho position having –CI and –Br (complex V and VI) substituent on benzyl ring decrease the LC_{50} value in brine shrimp assay. All the complexes have higher antibacterial activity against *B. substilis* except complex- IV, which has an electron releasing group attached to the ancillary ligand. Complexes (I and III) have potent antibacterial activity against *B. substilis* and *E. coli*. Complexes (I, II, and IV) have less percentage viability and complexes (III, V, VI) have higher percentage viability in *in vivo* cytotoxicity against *S. pombe* cells.

Figure 5. General structural-activity relationship of mixed ligand Pd(II) complexes for evaluation of LC_{50} value by brine shrimp lethality bioassay, antibacterial activity against two Gram(+ve) and three Gram(-ve), and *in vitro* cellular level bioassay against *S. pombe* cell.

3.6 DNA binding studies

3.6.1 Absorption titration study

The absorption titration method is one of the most useful tools for the investigation of the mode of interaction of synthesized compounds with HS-DNA. The absorption spectrum of hydrazinyl based Schiff base and their corresponding Pd(II) complexes at the constant concentration (125 µM) in the absence and presence of HS-DNA (0-500 µL) with different concentration is shown in Fig. 6. As shown in Fig. 6, when titrated by HS-DNA, the complexes presented significant hypochromism effect around 240-265 nm and accompanied the slightly red shifts in the absorbance maxima [40]. These spectral characteristics suggest that the complex may interact with HS-DNA through the intercalation mode. After the compounds intercalate to the base pairs of DNA, the π^* orbital of the intercalated compounds could couple with π orbital of the base pairs, hence decreasing the π-π^* transition energies, thus resulting in hypochromism. The hydrazinyl based Pd(II) complexes showed more hypochromicity than the ligands, indicating that the binding strength of the Pd(II) complexes is higher than the free ligands.

To quantitatively evaluate the binding affinity of the complexes with increasing DNA concentration, the intrinsic binding constant (K_b) was determined by monitoring the changes in absorbance at about 267-280 nm using the following equation.

$$[DNA]/\varepsilon_a-\varepsilon_f = [DNA]/(\varepsilon_b-\varepsilon_f) + 1/K_b(\varepsilon_b-\varepsilon_f)$$

where, ε_a, ε_f, and ε_b are the apparent extinction coefficients $A_{obs/[complex]}$, the extinction coefficient for the free complexes, and the extinction coefficient for the complexes in the fully bound form, respectively. [DNA] is the concentration of DNA in base pairs, and K_b is the intrinsic binding constant determined from the slop to intercept ratio of a plot of $[DNA]/\varepsilon_a-\varepsilon_f$ versus [DNA]. The K_b value of hydrazinyl based ligands and mixed-ligand Pd(II) complexes are found in the range of 0.10 - 0.83 × 10^5 M^{-1} and 1.10 - 1.89 × 10^5 M^{-1} respectively, which is comparable to the standard drug cisplatin, i.e. 5.51 × 10^4 M^{-1} and transplatin i.e. 1.75 × 10^4 M^{-1} and lower than classical intercalator EB, i.e. 7 × 10^7 M^{-1}. The binding strength of metal complexes with DNA is comparable to the reported complexes [22]. From the data, we can note that the chelation of ligand to metal enhances the binding affinity of the ligands. Percentage hypochromicity was calculated by [(A_{free}-A_{bound})/A_{free} × 100]. Hypochromism of hydrazinyl based ligands (L^1-L^6) and Pd(II) complexes (I-VI) are 9.20- 32.6% and 11.0-30.9%, respectively. The Gibb's free energies of the synthesized compounds are observed in the range of -22.81 to -30.07 $kJmol^{-1}$. The

binding constant (K_b) values of metal complexes with HS-DNA are found in increasing order of V > IV > VI > III >I > II. The binding constant (K_b), percentage hypochromism(%H) and Gibb's free energy data of the ligands (L^1-L^6), and metal complexes are represented in Table 1. All the ligands and metal complexes graph are represented in supplementary material 10.

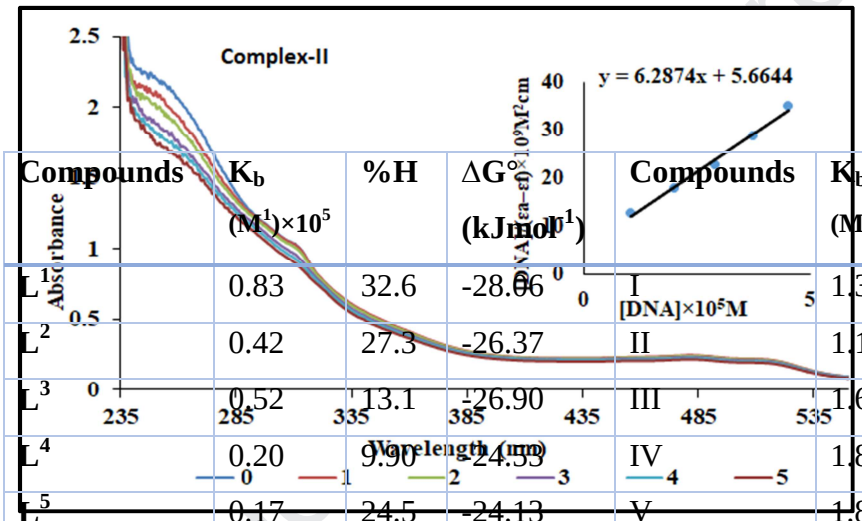

Table 1. Binding constant (K_b) and Gibb's free energy and percentage hypochromism (%H) of ligands (L^1-L^6) and Pd(II) complexes (I-VI).

Compounds	**K_b (M^{-1})×10^5**	**%H**	**ΔG° (kJmol^{-1})**	**Compounds**	**K_b (M^{-1})× 10^5**	**%H**	**ΔG° (kJmol^{-1})**
L^1	0.83	32.6	-28.06	I	1.37	11.0	-29.30
L^2	0.42	27.3	-26.37	II	1.10	28.8	-28.76
L^3	0.52	13.1	-26.90	III	1.63	26.8	-29.73
L^4	0.20	9.90	-24.53	IV	1.84	31.9	-30.03
L^5	0.17	24.5	-24.13	V	1.87	26.0	-30.07
L^6	0.10	23.3	-22.81	VI	1.81	30.9	-29.99

Figure 6. Absorption titration spectra of mixed ligand Pd(II) complex (II) (125 µM) with increasing concentration of HS-DNA (0-500 µM) in phosphate buffer (Na_2HPO_4/ NaH_2PO_4).

3.6.2 Fluorescence study

Ethidium bromide (EB) displacement is a useful method to examine the reactivity of chemical and biological systems it gives information about binding mechanisms and provides clues for the nature of binding. EB emits intense fluorescent light in the presence of DNA due to strong intercalation between the adjacent DNA base pairs. The intercalation of Pd(II) complexes with HS-DNA was monitored by studying the quenching the fluorescence of HS-DNA with increasing concentration of Pd(II) complexes. With the gradual increase of the concentration of complexes, the fluorescence intensity of DNA-EtBr gradually decreased as shown in Fig. 7. The displacement of EB by complexes at 610 nm suggests the intercalative mode of complex to DNA binding. The observed quenching of DNA-EB fluorescence by the complexes suggest that the complexes can significantly displace ethidium bromide from the DNA-EB system, thus illuminating the intercalation mode of binding [41, 42]. Ethidium bromide displacement data of Pd(II) complexes and graph are represented in supplementary material 11. This shows a dramatic increase in the fluorescence intensity of the EB-DNA by adding the Pd(II) complexes. The quenching plot illustrates that the fluorescence quenching of EB bound to DNA by the palladium (II) complexes is in linear agreement with the stern-Volmer relationship.

$$I_0/I = 1 + Ksv[Q]$$

where, I_0 and I represent the fluorescence intensities in the absence and presence of quencher, respectively. Ksv is a linear stern volmer quenching constant and [Q] is the concentration of quencher.

The Ksv value calculated from the plot of I_0/I versus [complex] is shown in Figure 7. The stern-Volmer quenching constant (Ksv), change in standard Gibb's free energy ($\Delta G°$), and binding constant (K_f) of palladium (II) coordination compounds are shown in Table 2, respectively. The K_f values calculated from the Scatchard plots indicate that the complex V displays the higher binding ability and the order of binding strength of the complexes to HS-DNA is V > IV > VI > III > I > II, which is the same as observed in the UV titration study.

Table 2. Linear stern volmer quenching constant (K_{sv}, M^{-1}), number of binding sites (n), associative binding constant ($K_{f,}$ M^{-1}) of mixed ligand Pd(II) complexes with HS-DNA.

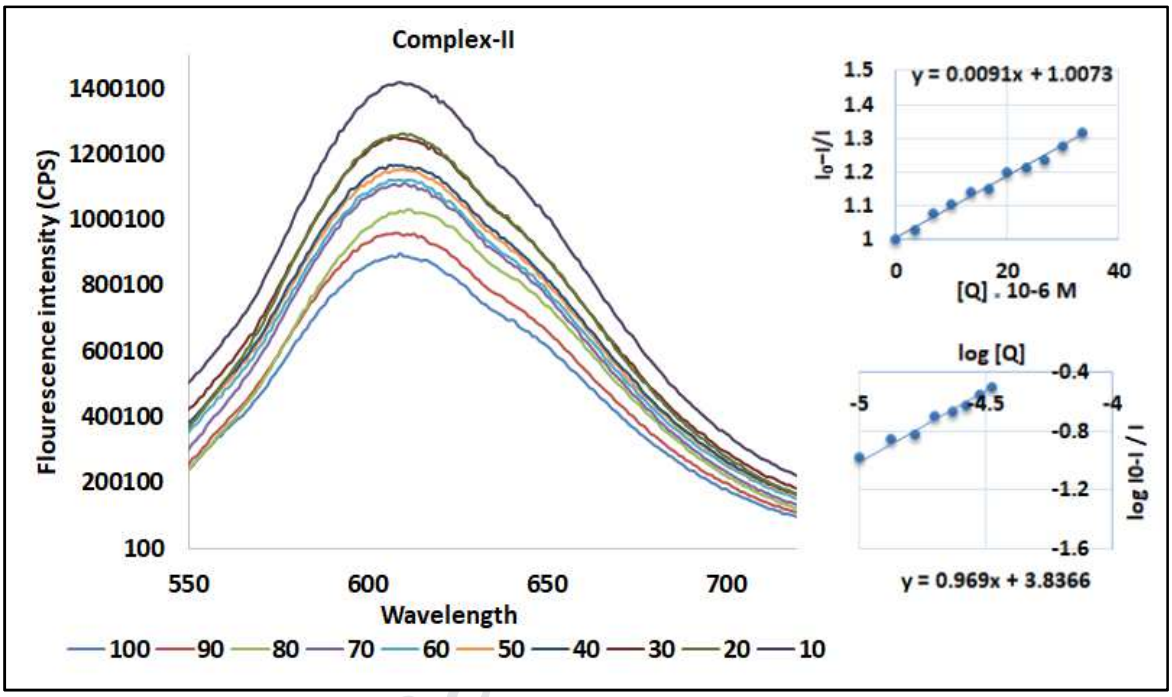

Figure 7. Fluorescence emission spectra of EtBr binds to HS-DNA in the absence and presence of compounds.

3.6.3 Effect of HS-DNA on hydrodynamic volume measurement

Complexes	K_{sv} (M^{-1})	Binding sites (n)	K_f (M^{-1})
I	5.3×10^3	1.138	2.1×10^4
II	9.1×10^3	0.969	0.6×10^4
III	7.7×10^3	1.148	3.5×10^4
IV	6.0×10^3	1.209	5.5×10^3
V	4.4×10^3	1.222	5.0×10^4
VI	6.7×10^3	1.208	6.8×10^3

Hydrodynamic volume measurements, such as viscosity of HS-DNA is critical test for evaluation of binding mode in solution in the absence of crystallographic structural data. Classical intercalation mode should result in lengthening the DNA helix as base pairs are separated to accommodate the binding ligand or the non-classical intercalation could bend or kink the DNA helix, thereby decreasing its length and viscosity [35]. From the viscosity

measurements, it was observed that there is an increase in the relative viscosity of the HS-DNA solution by increasing the concentration of complexes given in Fig. 8. The values of relative viscosity, $(\eta/\eta_0)^{1/3}$ (η_0 and η are the specific viscosity contributions of DNA in the absence and the presence of the complexes) were plotted against 1/R (R = [DNA]/[complex]). In the viscosity curve, the results reveal that the increasing concentration of metal complexes increases the viscosity of HS-DNA, which provide strong evidence for intercalation mode of binding [43]. Thus, we may deduce that the mentioned complex can be considered as a DNA intercalator.

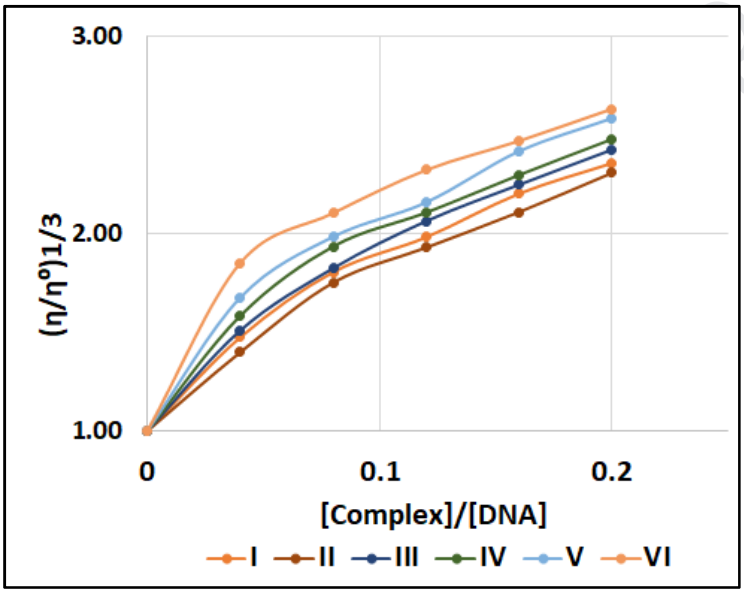

Figure 8. Effect of an increasing amount of mixed ligand Pd(II) complexes on the relative viscosity of HS-DNA at 27 °C, [DNA] = 200 µM. The results are the triplicate experiments carried out under identical conditions.

3.6.4 Computational study

Molecular docking is an attractive scaffold to understand drug biomolecular interactions for the rational drug design. The information about the docking technique can be employed to suggest the binding energy, stability of complexes, and to predict the tentative binding parameters of the ligand-receptor complex. The molecular docking results exhibit the ligands and their corresponding Pd(II) complexes approach the DNA cleavage site forming stable complexes through the intercalation mode of binding. The relative binding energy of

the docked structures of ligands is -210.14 (L^1), -211.27 (L^2), -195.52 (L^3), -205.43 (L^4), -204.72 (L^5), -196.05 (L^6) kJ $mol^{-1}$and complexes are -257.48 (I), -259.71 (II), -258.08 (III), -244.63 (IV), -254.68 (V), -241.37 (VI) kJ mol^{-1}. The representative docked structure is shown in Fig. 9 and other structures are shown in supplementary material 12.

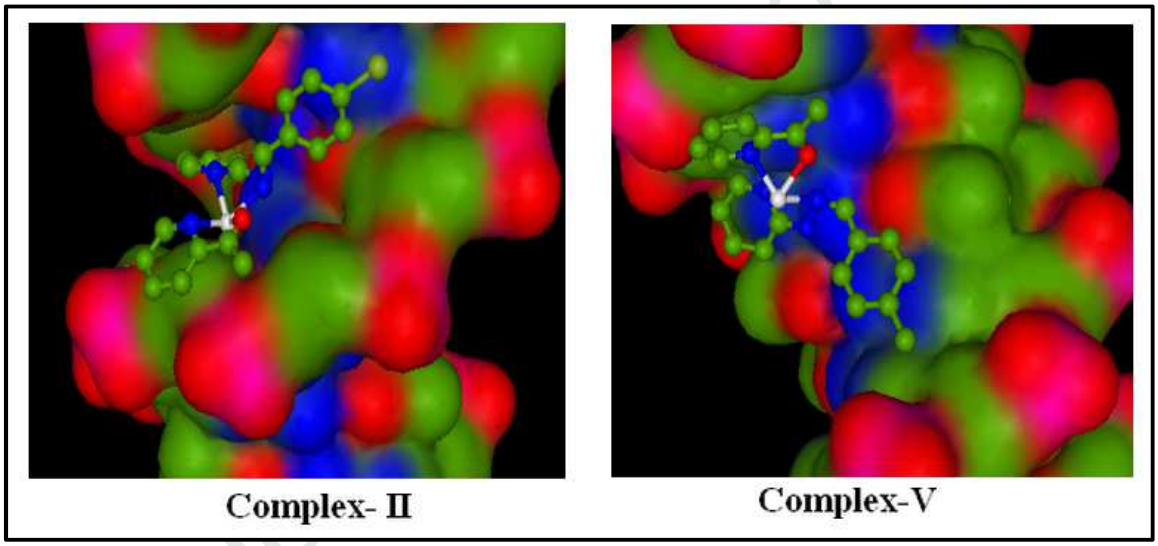

Figure 9. Molecular docking study of mixed ligand Pd(II) complexes (II and V) with DNA helix (PDB ID: 1BNA).

3.6.5 Photochemical analysis of DNA nuclease activity

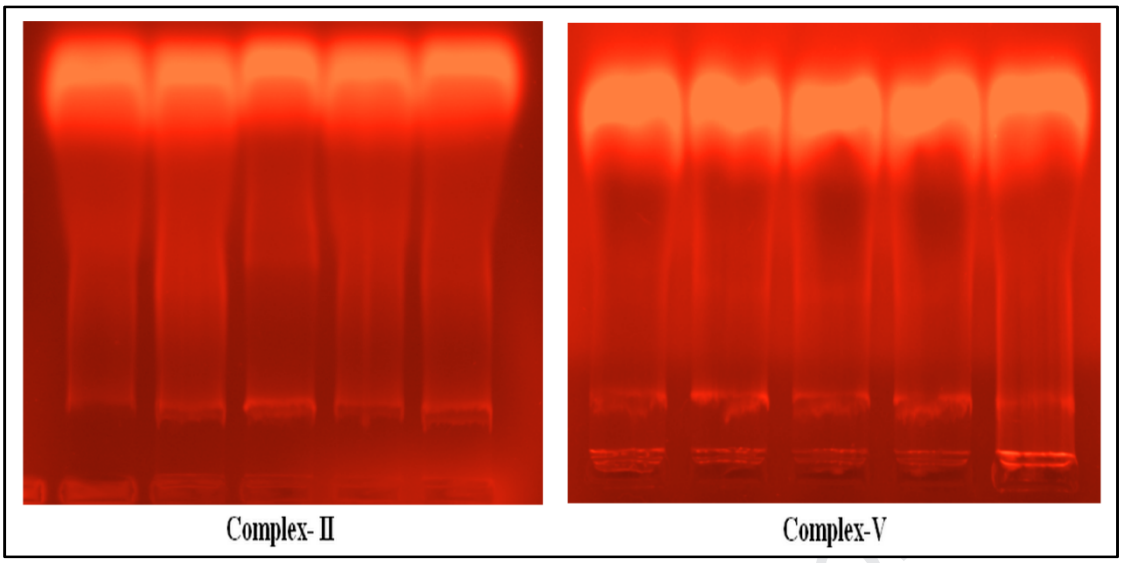

Figure 10. DNA damage of the *S. pombe* cells by the treatment of complex (II and V) in the range of (20-100 µM).

The electrophoresis experiment was performed to monitor the outcome of DNA nuclease activity against stimulated *S. pombe* cell to see whether the complexes have any consequence on the degradation of DNA or not. The study of DNA cleavage efficiency of the molecule was examined by agarose gel electrophoresis. The treated and untreated *S. pombe* cells were separated from DNA for DNA degradation analysis of *S. pombe* cells. The damage caused by complex on DNA can be seen as DNA smearing due to the toxic nature of the compound, whereas control cell DNA appeared normal as an intact band. Smearing of DNA in Pd(II) complexes concluded that the damage occurs because of the toxic nature of the compounds (Fig. 10). The results suggest complexes as a good genotoxic agent, data of DNA cleavage of all Pd(II) complexes is shown in supplementary material 13.

3.7 Protein binding study

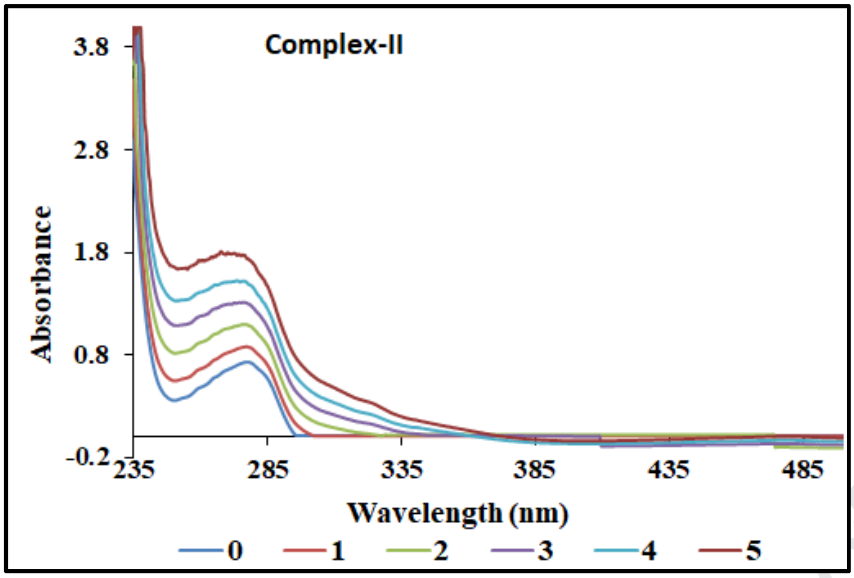

Figure 11. UV-absorption spectra of BSA (15 µM) in the presence different concentration of complexes (0- 40 µM).

UV- vis absorption spectroscopy is a common method to explore the structural changes of protein and investigate protein complex formation. Static and dynamic quenching can be distinguished by UV-absorption spectroscopy, which is done by the absorption spectra of BSA in the presence of complexes. The UV absorption spectra of BSA in the presence and absence of complexes revealed that the absorption intensity of BSA was enhanced as the concentration of the compounds increased, and there was a little blue shift for all compounds [44, 45]. Fig. 11 indicates that upon adding the complexes, BSA skeleton absorption intensity decrease in the range of 278-283 nm and blue shift appear due to the perturbation of the secondary structure of the protein. Pd(II) complexes absorption titration graph with BSA is represented in supplementary material 14.

4. Conclusion

The novel mixed-ligand Pd(II) complexes(I-VI) were synthesized by the complexation of hydrazinyl pyridine based substituted Schiff base (L^1-L^6), 2-acetyl pyridine with Na_2PdCl_4. Spectroscopic characterization (UV-vis, ^{1}H NMR, ^{13}C NMR, and mass) supported the formation of the complexes. The Pd(II) complexes having square planar geometry, diamagnetic nature, and d^8-low spin configuration with dsp^2 hybridization. The structure

optimization of complexes suggest that pyridine rings of both the ligands are cis to each other. The UV-visible spectral titration for protein binding study suggests perturbation in the secondary structure of protein influenced by Pd(II) complexes. The UV-visible, viscosity, fluorescence titration and molecular docking studies of Pd(II) complexes reveal that the interaction of synthesized complexes with HS-DNA is specifically through intercalation type of binding. The synthesized Pd(II) complexes have potent antimicrobial activity against Gram(+ve) and Gram(-ve) bacterial species than the Schiff bases. All the mixed-ligand Pd(II) complexes exhibit good *in vitro* cytotoxic activity and cellular level cytotoxicity.

ACKNOWLEDGMENT

The authors are thankful to the Head, Department of Chemistry, Sardar Patel University, for providing necessary research facilities; DST-PURSE Sardar Patel University, for LC-MS analysis; CAS-Phase-II and UGC-CPEPA program, Sardar Patel University for providing instrumental and chemicals facilities.

Reference

[1] M. Yousefi, T. Sedaghat, J. Simpson, M. Shafiei, Applied Organometallic Chemistry, 33 (2019) e5137.

[2] G. Ayyannan, P. Veerasamy, M. Mohanraj, G. Raja, A. Manimaran, M. Velusamy, N. Bhuvanesh, R. Nandhakumar, C. Jayabalakrishnan, Applied Organometallic Chemistry, 31 (2017) e3599.

[3] K. Karami, N. Jamshidian, M. Zakariazadeh, Applied Organometallic Chemistry, 33 (2019) e4728.

[4] P. ČAnoviĆ, J. Bogojeski, S. MarkoviĆ, M. Zivanovic, Turkish Journal of Biology, 41 (2017) 141-147.

[5] W.H. Mahmoud, G.G. Mohamed, M.M. El-Dessouky, Journal of Molecular Structure, 1082 (2015) 12-22.

[6] F.P. Andrew, P.A. Ajibade, Journal of Molecular Structure, 1155 (2018) 843-855.

[7] N. Şahin, S. Şahin-Bölükbaşı, M.N. Tahir, C. Arıcı, E. Çevik, N. Gürbüz, İ. Özdemir, B.S. Cummings, Journal of Molecular Structure, 1179 (2019) 92-99.

[8] O. Kacar, B. Cevatemre, I. Hatipoglu, N. Arda, E. Ulukaya, V.T. Yilmaz, C. Acilan, Bioorganic & Medicinal Chemistry, 25 (2017) 1770-1777.

[9] M. Milutinović, M. Stanković, D. Cvetković, V. Maksimović, B. Šmit, R. Pavlović, S. Marković, Journal of Food Biochemistry, 39 (2015) 238-250.

[10] J. Zhang, X. Wang, C. Tu, J. Lin, J. Ding, L. Lin, Z. Wang, C. He, C. Yan, X. You, Z. Guo, Journal of Medicinal Chemistry, 46 (2003) 3502-3507.

[11] M.P.M. Marques, ISRN Spectroscopy, 2013 (2013) 29.

[12] S.A. Hosseini, M. Eslami Moghadam, M. Saeidifar, A.A. Saboury, Canadian Journal of Physiology and Pharmacology, 96 (2018) 1276-1285.

[13] A.A. Adeniyi, P.A. Ajibade, Bioinorganic Chemistry and Applications, 2018 (2018) 12.

[14] L. Giovagnini, L. Ronconi, D. Aldinucci, D. Lorenzon, S. Sitran, D. Fregona, Journal of Medicinal Chemistry, 48 (2005) 1588-1595.

[15] A.M. Abu-Dief, I.M.A. Mohamed, Beni-Suef University Journal of Basic and Applied Sciences, 4 (2015) 119-133.

[16] J. Ruiz, N. Cutillas, C. Vicente, M.D. Villa, G. López, J. Lorenzo, F.X. Avilés, V. Moreno, D. Bautista, Inorganic Chemistry, 44 (2005) 7365-7376.

[17] K. Karami, Z.M. Lighvan, S.A. Barzani, A.Y. Faal, M. Poshteh-Shirani, T. Khayamian, V. Eigner, M. Dušek, New Journal of Chemistry, 39 (2015) 8708-8719.

[18] C. Icsel, V.T. Yilmaz, Y. Kaya, H. Samli, W.T.A. Harrison, O. Buyukgungor, Dalton Transactions, 44 (2015) 6880-6895.

[19] R.R. Varma, B.H. Pursuwani, E. Suresh, B.S. Bhatt, M.N. Patel, Journal of Molecular Structure, 1200 (2020) 127068.

[20] M. Frisch, G. Trucks, H. Schlegel, G. Scuseria, M. Robb, J. Cheeseman, G. Scalmani, V. Barone, B. Mennucci, G. Petersson, Wallingford, CT, 32 (2009) 5648-5652.

[21] A.F. Santos, D.F. Brotto, L.R.V. Favarin, N.A. Cabeza, G.R. Andrade, M. Batistote, A.A. Cavalheiro, A. Neves, D.C.M. Rodrigues, A. dos Anjos, Revista Brasileira de Farmacognosia, 24 (2014) 309-315.

[22] K.P. Thakor, M.V. Lunagariya, B.S. Bhatt, M.N. Patel, Luminescence, 34 (2019) 113-124.

[23] K. Ghazal, S. Shoaib, M. Khan, S. Khan, M. Rauf, N. Khan, A. Badshah, M. Tahir, A. Irshad, A. Rehman, Journal of Molecular Structure, 1177 (2019) 124-130.

[24] I. Aziz, M. Sirajuddin, S. Nadeem, S.A. Tirmizi, Z. Khan, A. Munir, K. Ullah, B.A. Farooqi, H. Khan, M.N. Tahir, Russian Journal of General Chemistry, 87 (2017) 2073-2082.

[25] D.A. Kanthecha, B.S. Bhatt, M.N. Patel, Heliyon, 5 (2019) e01968.

[26] S. Gopu, V. Ravi kumar, K. Laxma Reddy, P. Venkat Reddy, S. Sirasani, Nucleosides, Nucleotides and Nucleic Acids, 38 (2019) 349-373.

[27] X.-W. Li, X.-H. Zhao, Y.-T. Li, Z.-Y. Wu, Inorganica Chimica Acta, 488 (2019) 219-228.

[28] A. Heydari, H. Mansouri-Torshizi, RSC Advances, 6 (2016) 96121-96137.

[29] N.J. Patel, B.S. Bhatt, M.N. Patel, Inorganica Chimica Acta, 498 (2019) 119130.

[30] K. Karami, Z. Mehri Lighvan, A.M. Alizadeh, M. Poshteh-Shirani, T. Khayamian, J. Lipkowski, RSC Advances, 6 (2016) 78424-78435.

[31] L.H. Abdel-Rahman, M.S.S. Adam, A.M. Abu-Dief, H. Moustafa, M.T. Basha, A.S. Aboraia, B.S. Al-Farhan, H.E.-S. Ahmed, Applied Organometallic Chemistry, 32 (2018) e4527.

[32] E.A. Popova, A.V. Protas, A.V. Mukhametshina, G.K. Ovsepyan, R.V. Suezov, A.V. Eremin, E.I. Stepchenkova, E.R. Tarakhovskaya, A.V. Fonin, G.L. Starova, Polyhedron, 158 (2019) 36-46.

[33] B.T. Khan, K.M. Mohan, G.N. Goud, Indian Journal of Chemistry - Section A, 31A (1992) 28-33.

[34] A.A. Franich, M.D. Živković, D. Ćoćić, B. Petrović, M. Milovanović, A. Arsenijević, J. Milovanović, D. Arsenijević, B. Stojanović, M.I. Djuran, JBIC Journal of Biological Inorganic Chemistry, 24 (2019) 1009-1022.

[35] K.P. Thakor, M.V. Lunagariya, B.S. Bhatt, M.N. Patel, Applied Organometallic Chemistry, 32 (2018) e4523.

[36] K.B. Choo, W.L. Mah, S.M. Lee, W.L. Lee, Y.L. Cheow, Applied Organometallic Chemistry, 32 (2018) e4377.

[37] K.P. Thakor, M.V. Lunagariya, B.S. Bhatt, M.N. Patel, Monatshefte für Chemie - Chemical Monthly, 150 (2019) 233-245.

[38] L. Liu, H. Gao, H. Wang, Y. Zhang, W. Xu, S. Lin, H. Wang, Q. Wu, J. Guo, Oncology letters, 14 (2017) 3741-3747.

[39] B.S. Bhatt, D.H. Gandhi, F.U. Vaidya, C. Pathak, T.N. Patel, Journal of Biomolecular Structure and Dynamics, (2020) 1-10.

[40] R. Kumari, M. Nath, Applied Organometallic Chemistry, 32 (2018) e4365.

[41] L.-L. Lv, W.-M. Xia, Y.-Z. Cheng, L.-P. Zhang, X.-D. Wang, in: Main Group Metal Chemistry, 2019, pp. 60.

[42] B.G. Gowda, International Journal of Pharmacy and Pharmaceutical Sciences, 6 (2014) 607-609.

[43] M. Kumar, G. Kumar, K.M. Dadure, D.T. Masram, New Journal of Chemistry, 43 (2019) 15462-15481.

[44] X. Pan, P. Qin, R. Liu, J. Wang, Journal of Agricultural and Food Chemistry, 59 (2011) 6650-6656.

[45] R. Prabhakaran, P. Kalaivani, P. Paramasivan, F. Dallemer, R. Huang, V. Padma, K. Natarajan, Bioorganic & Medicinal Chemistry, 21 (2013) 8323-8332.

Highlights

- Six different mixed ligand Pd(II) complexes were synthesized
- Intercalation mode of binding of complexes with the DNA helix
- Significant antibacterial and anticancer activity was found for the complexes.
- Promising *in vitro* cytotoxicity against brine shrimp lethality bioassay.
- Cell proliferation inhibiting activity by MTT assay.

Declaration of interests

☒ The authors declare that they have no known competing financial interests or personal relationships that could have appeared to influence the work reported in this paper.

☐The authors declare the following financial interests/personal relationships which may be considered as potential competing interests: